Available online at www.sciencedirect.com

ScienceDirect

Energy Procedia 57 (2014) 255 – 264

Energy Procedia

2013 ISES Solar World Congress

Experimental and numerical study of a parabolic trough linear CPVT system

Davide Del Col, Matteo Bortolato, Andrea Padovan, Michele Quaggia

Dipartimento di Ingegneria Industriale, Università degli Studi di Padova, Via Venezia 1, Padova, 35131, Italy
E-mail:davide.delcol@unipd.it

Abstract

The electric and thermal performance of a parabolic trough linear concentrating photovoltaic-thermal (CPVT) system operating in Padova (northern Italy) is experimentally investigated. The system moves about two axes and exhibits a geometrical concentration ratio around 130. The receiving module placed on the focus line displays a secondary optics made of two flat mirrors to gather some reflected radiation and to contribute to the concentrated flux on two lines of triple junction photovoltaic cells soldered on a ceramic substrate. The substrate is in thermal contact with a aluminium heat exchanger with water flow channels to cool the PV cells.
During the test runs, the inlet water temperature ranges from 20°C to 80°C and the heat yield is obtained from mass flow rate and temperature measurements while a rheostat and a power analyzer are connected to the electric terminals of the module to assess the electrical production. The direct normal irradiation (DNI) is measured by a pyrherliometer mounted on a solar tracker. Experimental results are used to assess a numerical model of the solar receiver and the whole concentrator.

Keywords:CPVT system; parabolic trough

1. Introduction

Flat-plate crystalline silicon modules display an efficiency decrease when increasing the operating temperature of the cells. The efficiency penalization can be reduced by cooling the photovoltaic cells; depending on the temperature of the cooling fluid, sometimes heat can also be recovered. However, as shown by Del Col et al. [1], the thermal efficiency of flat-plate photovoltaic-thermal modules quickly decreases with increasing temperature of the cooling fluid and such devices can respond to the heat demand only for low temperature applications, such as swimming pools and domestic hot water in summer months. Reasons of the limited thermal performance can be searched in the low density power on the cells and the high frontal area exposed to the heat dissipations.

doi:10.1016/j.egypro.2014.10.030

In concentrating photovoltaic systems (CPV), cooling of the PV cells is necessary because otherwise an excessive temperature may lead to irremediable damages [2]. In the case of point focus solar concentration, a natural convection passive cooling system consisting of finned surfaces exposed to the air is generally employed. Solar concentrators with linear focus are suitable for the use of active cooling of PV cells and, if heat recovery is performed, they are regarded as concentrating photovoltaic-thermal (CPVT) systems. As compared to flat-plate devices, CPVT systems exhibit characteristics more suitable for the cogeneration of electrical energy and heat. Besides, they could meet the heat demand at medium temperature, which is very interesting because the value of heat increases with increasing temperature of utilization.

Nomenclature

A	surface area (m^2)
a	photovoltaic model curve fitting parameter (V)
A_m	projected area of the mirrors (m^2)
c_p	specific heat of the water ($J\ kg^{-1}\ K^{-1}$)
DNI	direct normal irradiance ($W\ m^{-2}$)
E	voltage (V)
HE	heat exchanger
I	current generated by the photovoltaic cells (A)
I_0	diode reverse saturation current (A)
I_L	light current (A)
m_W	water mass flow rate ($kg\ s^{-1}$)
P_{el}	electrical power (W)
q_{th}	useful heat flow rate (W)
R_{el}	electrical resistance (Ω)
R_{th}	thermal resistance ($m^2\ K\ W^{-1}$)
t	time (s)
T	temperature (°C)
T_m^*	reduced temperature difference ($K\ m^2\ W^{-1}$) $= [(T_{W,out} + T_{W,in}) / 2 - T_{amb}] / DNI$
V	volume (m^3)
Greek symbols	
η	global efficiency (-)
η_{el}	electrical efficiency (-)
η_{th}	thermal efficiency (-)
ρ	density ($kg\ m^{-3}$)

Subscripts

A	ceramic substrate
amb	ambient air
C	cells
G	glass
i	i-th element of the module
in	inlet mixing point
out	outlet mixing point
s	series
sh	shunt
W	water

A new CPVT prototype, set up at Dipartimento di Ingegneria Industriale, University of Padova, in northern Italy, is hereafter presented and described. As compared to most existing low concentration systems with linear focus, which use silicon crystalline cells, as reported in the review paper by Chemisana [3], the module installed in the present system is composed of triple junction solar cells. Multi-junction solar cells exhibit a limited dependence of efficiency on the operating temperature and can work with good efficiency even at 100°C, as shown for example by Pérez-Higueras et al. [4]. This allows heat production at medium temperature when active cooling is used.

A model of the photovoltaic-thermal module is developed to describe the behaviour in steady-state and dynamic conditions. Simulations of daily production of electrical energy and heat are reported and discussed.

2. CPVT prototype

The new prototype of linear photovoltaic concentrator is shown in Figure 1. Four parabolic trough mirrors concentrate the solar radiation onto a linear receiver 2.4 m long, where a photovoltaic-thermal module is placed. The aperture area of the present system is 6.857 m^2 and the geometrical concentration ratio is nearly 130. The device has a modular arrangement and more modules could be added by increasing the number of mirrors and the length of the receiver. The system moves about two-axes (azimuthal and zenithal motions), to have the beam radiation normal to the plane. The motion is governed by a solar algorithm when approaching the sun and by a solar sensor when achieving the best receiver alignment.

The photovoltaic-thermal module is shown in Figure 2 and it is the test section in the present work. A secondary optics device, composed of flat aluminium mirrors, has been designed for reducing optical losses. The module is equipped with GaInP/GaAs/Ge triple junction solar cells soldered on a ceramic substrate, which in turn is in thermal contact with an active cooling system including an aluminium roll-bond heat exchanger and a closed loop for pumping water as the coolant. The roll-bond plate is applied to the back side and drowned into an elastomeric material. The PV cells have a square shape with side length equal to 10 mm and are electrically connected to form a package of 22 cells. Each PV package has an efficiency of 34.6% at 25°C cell temperature, 1000 W m^{-2} *DNI*, 1.5 air mass and 120 concentration ratio, as reported by the manufacturer. The module is long 1.2 m and is composed of ten PV packages.

Fig. 1. CPVT prototype during tests at University of Padova

Fig. 2. Photovoltaic-thermal module.

3. Test facility

A scheme of the hydraulic loop built up at the Dipartimento di Ingegneria Industriale to test the solar concentrator is reported in Fig. 3. The water coming from the active cooling system of the photovoltaic cells enters the storage 1 and then passes through a plate heat exchanger that acts as a heat sink. The water enters the storage 2, which contains four electrical heaters for the temperature regulation. According to the operating mass flow rate, it is possible to set the electric power to obtain a desired and constant temperature of the liquid at the inlet of the test section. From storage 2 the water is pumped through a Coriolis effect mass flow meter before entering the heat exchanger of the module. The inlet and outlet water temperatures in the test section and the ambient air temperature are measured by means of PT100 platinum resistance thermometers.

The electrical terminals of the module are connected to a rheostat and a power analyzer that measures the current of the circuit, the voltage across the resistive load and the electrical power supplied by the PV cells. During the test runs, the sliding contact of the rheostat is set in order to make the PV module work close to the maximum power point. The laboratory is equipped with a measuring system of solar irradiance, composed of a secondary standard pyranometer for the measurement of horizontal global irradiance, a secondary standard pyranometer shaded with a band for the measurement of the horizontal diffuse irradiance and a pyrheliometer mounted on a sun tracker for measuring the direct normal irradiance (DNI).

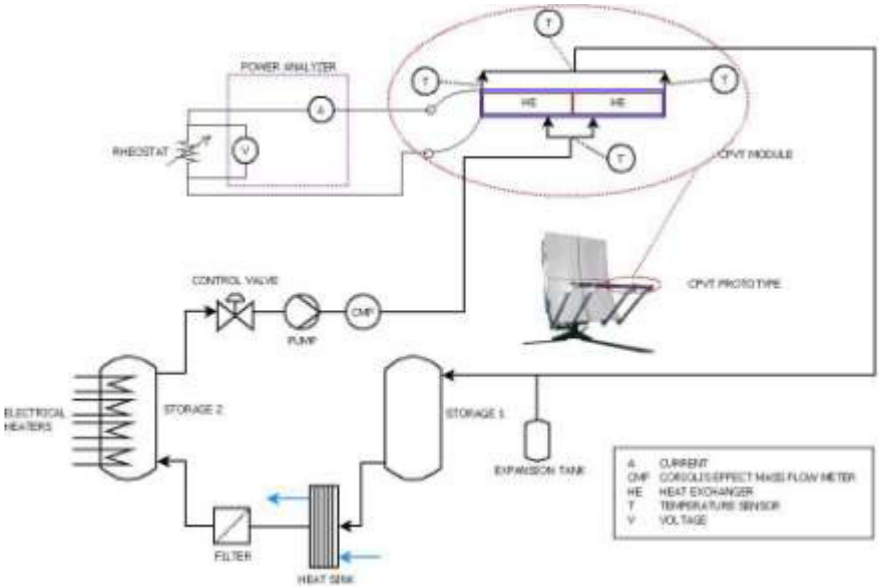

Fig. 3. Schematic view of the experimental test rig.

4. Data reduction

In order to characterize the thermal performance of the CPVT prototype, the mass flow rate, the inlet and outlet temperatures of the working fluid and the ambient air temperature are measured, together with DNI, global and diffuse horizontal irradiance. It is worthy to point out that, as reported by Vivar et al. [5], there are no appropriate standard procedures for testing and qualifying concentrated photovoltaic-thermal devices with active cooling system. The steady-state method described in the standard EN 12975-2 [6] is adopted here for the present experimental tests. In the specifications, the direct normal irradiance is considered instead of the global irradiance on the collector plane because it is the actual input energy flux of the studied solar concentrator. The mass flow rate is set equal to 260 kg h^{-1}, in compliance with the stated fluid flow rate of 0.02 kg s^{-1} per square metre of the aperture area. Measurements are repeated at varying inlet water temperature. After exiting the test section, the water temperature is measured at the outlet of each hydraulic circuit integrated in the heat exchanger and at the mixing point.

Test runs have been performed both in open electric circuit conditions and with electric load, by connecting the rheostat and the power analyzer to the electrical terminals of the module. In the latter case, with electric load, the power analyzer measures the current generated by the photovoltaic cells, the voltage across the resistive load and the supplied power. The sliding contact of the rheostat is set close to the maximum power point by observing the electrical power output trend and the proper position is manually checked several times during each test run.

During steady-state test conditions, measurements are collected to produce a set of thermal efficiency data points:

$$\eta_{th} = \frac{q_{th}}{DNI \cdot A_m} = \frac{\dot{m}_W \cdot c_{p,W} \cdot \left(T_{W,out} - T_{W,in}\right)}{DNI \cdot A_m} \quad (1)$$

The thermal performance of the concentrator is described plotting thermal efficiency as a function of the reduced temperature difference T_m^*. When the rheostat and the power analyzer are electrically connected to the module, the electrical efficiency can be calculated according to Eq. (3):

$$\eta_{el} = \frac{P_{el}}{DNI \cdot A_m} = \frac{E \cdot I}{DNI \cdot A_m} \qquad (2)$$

and considering the useful heat flow rate and the electric power provided by the CPVT prototype, the global efficiency of the investigated system can be defined as follows:

$$\eta = \frac{q_{th} + P_{el}}{DNI \cdot A_m} \qquad (3)$$

Table 1: Experimental uncertainty of the measured parameters.

Measured parameter	Uncertainty
Water temperature	± 0.04 K at 5°C to ± 0.1 K at 90°C
Ambient air temperature	± 0.05°C
Mass flow meter	± 0.1%
Current	± 0.3%
Voltage	± 0.3%
Direct normal irradiance	± 2.5% at 900 W m^{-2}

The experimental analysis of the measured parameters has been done in agreement with the guidelines provided by the standard ISO Guide to the Expression of Uncertainty in Measurement [7]. In Table 1, the uncertainty of the measured parameters is reported with a level of confidence of 95%. In the case of thermal and electrical efficiency, which are not directly measured, the uncertainty is calculated with the law of uncertainty propagation.

5. Experimental results

The operating conditions of the present experimental data are: mass flow rate equal to 0.02 kg s^{-1} per square meter of projected area of the parabolic trough mirrors, *DNI* between 700 W m^{-2} and 950 W m^{-2}, ambient temperature between 15°C and 29°C. When performing tests runs in open electric circuit conditions, the water inlet temperature is set at around 20°C, 40°C and 45°C. With electric load, the simultaneous production of useful heat flow rate and electrical power is investigated by sending water to the test section at inlet temperature of 20°C, 70°C and 80°C.

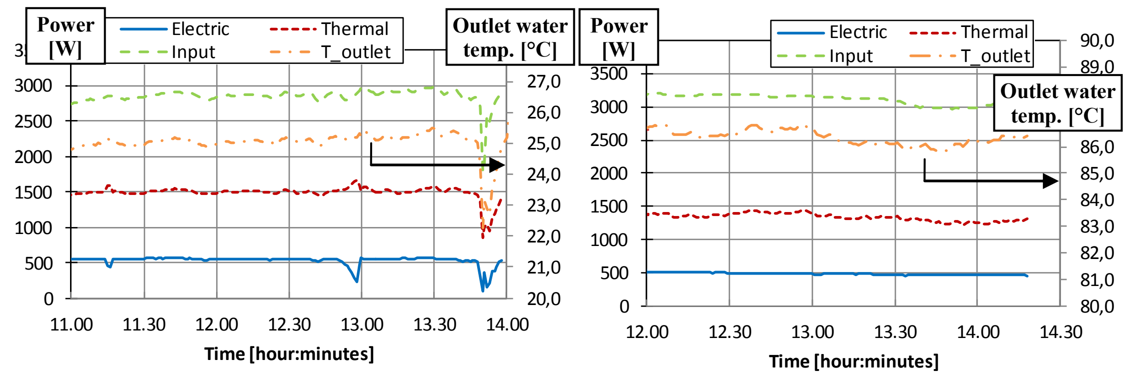

a) b)

Figure 4. Experimental data vs time of the day for two different test runs a) low water temperature; b) high water temperature.

The graph in Figure 4a) refers to the collected data during a test run displaying an outlet water temperature of around 25°C, with the rheostat and the power analyzer connected to the electrical terminals of the module. The input power, given by the *DNI* multiplied by the projected area of the mirror, the useful heat flow rate and the electrical power gained from the module are plotted against the time of the test day. The outlet water temperature is also plotted. Figure 4b) reports the same graph referred to a test run with electrical production and useful heat recovery and water outlet temperature of around 86°C.

Even though the input power is slightly higher during the test runs with water outlet temperature around 86°C, the thermal production moderately decreases because the heat losses towards the external environment increase with the fluid working temperature and the electrical efficiency diminishes due to the higher working temperature of the photovoltaic cells. The peculiar properties of the triple junction photovoltaic cells employed in the present concentrator allow the electrical power to remain around 500 W per module even at the higher temperature. With regard to the thermal performance, the small area of the module limits the heat losses.

This trend in thermal performance has been observed also in the test in open electrical circuit conditions. In Figure 5a and 5b, the input power and the useful heat flow rate are reported against the time of the day for two different test in which the water inlet temperature was set equal to 20°C and 40°C, respectively. From the comparison between Figure 4a and Figure 5a, one can notice that when running the CPVT system without electrical load and water inlet temperature of 20°C, the thermal production increases by the amount corresponding to the not performed electric production.

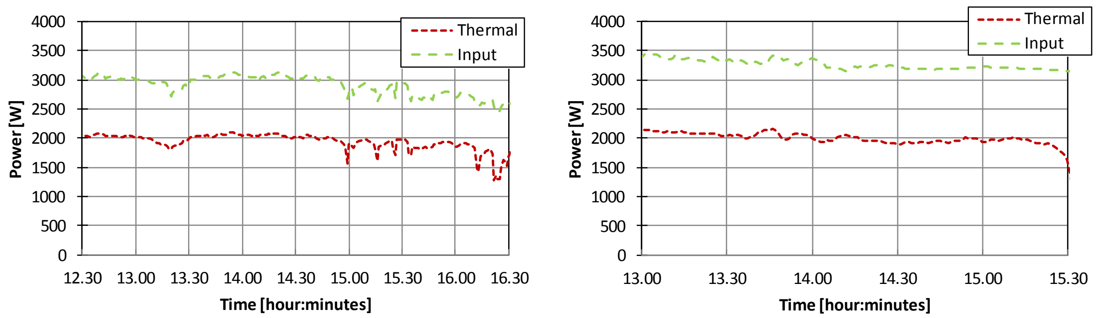

a) b)

Figure 5. Input power and useful heat flow rate without electric load at two inlet water temperatures: a) 20°C ; b) 40°C.

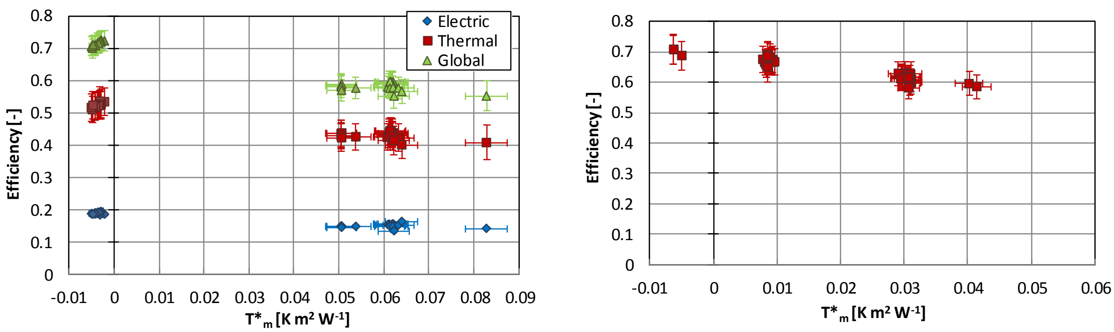

a) b)

Figure 6. Efficiency vs. reduced temperature difference during tests: a) with electric load; b) without electrical load.

In order to describe the performance of the present linear concentrator, thermal efficiency, electrical efficiency and global efficiency, measured during test runs with electric load, have been reported in Figure 6a) as a function of the reduced temperature difference T_m^*. In Figure 6b), the thermal efficiency obtained in test runs without electrical load is plotted against T_m^*. In agreement with the previous considerations, the thermal and electrical efficiency decrease when increasing the reduced temperature difference. This means that for a given DNI and ambient air temperature, the thermal and electrical performance of the investigated device decreases when increasing the mean temperature of the working fluid. On the whole, the global efficiency ranges between 0.7 and 0.55 when the reduced temperature difference T_m^* varies between 0 and 0.082 K m^2 W^{-1}.

6. Thermal and electrical model

The PV-T module is modelled by means of a lumped capacitance scheme, developed in Matlab/Simulink environment. Figure 7 shows the scheme of the module and the equivalent lumped capacitance model. The device has a multi-layer composition and four main nodes are used in the model: glass, PV cells, ceramic substrate, heat exchanger. The ceramic substrate is the layer where the PV cells are welded and ensures electrical insulation. Water flowing in single-phase is used as cooling fluid. The water node is connected only to the heat exchanger.

Eqs .(4) to (8) report the thermal balances associated with each node. As described in Duffie and Beckman [8], the electric model is based on Eq.(9), which is the I-V characteristic of the PV package.

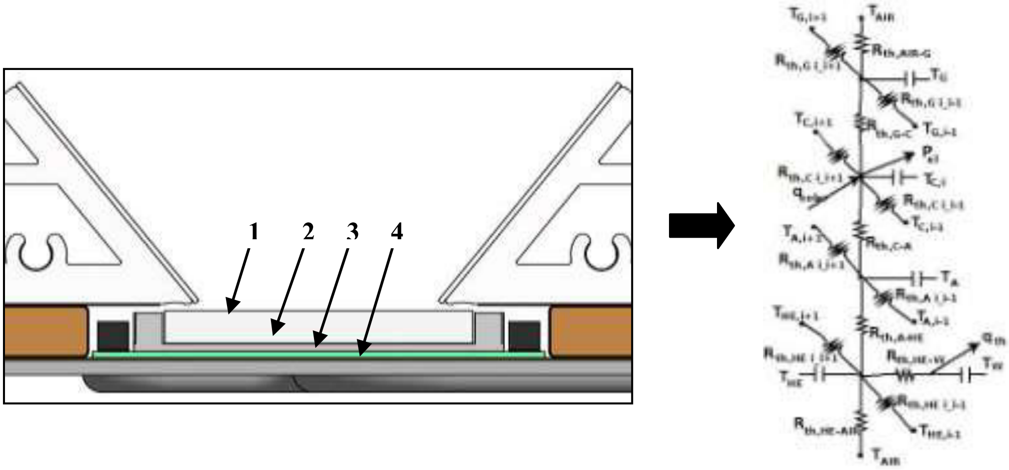

Figure 7. Scheme of the module (1: glass, 2: cells, 3:ceramic layer and 4: heat exchanger) and equivalent lumped capacitance model.

$$\rho_G V_{G,i} c_{p,G} \frac{\partial T_{G,i}}{\partial t} = \frac{1}{R_{th,AIR-G}} A_G \left(T_{AIR} - T_G\right) + \frac{1}{R_{th,G-C}} A_C \left(T_C - T_G\right) \tag{4}$$

$$\rho_C V_{C,i} c_{p,C} \frac{\partial T_{C,i}}{\partial t} = \frac{1}{R_{th,G-C}} A_C \left(T_G - T_C\right) + \frac{1}{R_{th,C-A}} A_C \left(T_A - T_C\right) + DNI \eta_{opt} A_m - P_{el} \tag{5}$$

$$\rho_A V_{A,i} c_{p,A} \frac{\partial T_{A,i}}{\partial t} = \frac{1}{R_{th,C-A}} A_C \left(T_C - T_A\right) + \frac{1}{R_{th,A-HE}} A_A \left(T_{HE} - T_A\right) \tag{6}$$

$$\rho_{HE} V_{HE,i} c_{p,HE} \frac{\partial T_{HE,i}}{\partial t} = \frac{1}{R_{th,A-HE}} A_A \left(T_A - T_{HE}\right) + \frac{1}{R_{th,HE-W}} A_W \left(T_W - T_{HE}\right) + \frac{1}{R_{th,HE-AIR}} A_{HE} \left(T_{AIR} - T_{HE}\right) \tag{7}$$

$$\rho_W V_{W,i} c_{p,W} \frac{\partial T_{W,i}}{\partial t} = \frac{1}{R_{th,HE-W}} A_W \left(T_{HE} - T_W\right) + \dot{m}_W c_{p,W} \left(T_{W,i,out} - T_{W,i,in}\right) \tag{8}$$

$$I = I_L - I_0 \left[e^{\frac{E + I R_{el,s}}{a}} - 1 \right] - \frac{E + I R_{el,s}}{R_{el,sh}} \tag{9}$$

In the present analysis the module has been divided along the flow direction in elementary sections, each 50 mm long, and energy balances are performed for each element. The water temperature at the outlet of the first element is then set equal to the temperature entering the second element and so on. A CFD analysis has been done to determine the heat transfer coefficients to be used in the numerical model. The model also includes conduction heat transfer along the flow direction; this terms are omitted in the equation balances, here reported, for the sake of simplicity. The optical efficiency of the concentrating system is equal to 0.7 and is obtained from a ray tracing study.

7. Results of simulations

Figure 8 is a comparison of the efficiencies calculated with the present model with those determined from the measurements. The graph on the left (Figure 8a) shows data measured with electric load: the electric curve of the model overestimates the experimental electric production because of some manufacturing defects, which eventually affect the agreement between experimental and predicted global efficiency. The graph on the right shows the efficiency measured when the electric load is not connected, and heat is the only useful output.

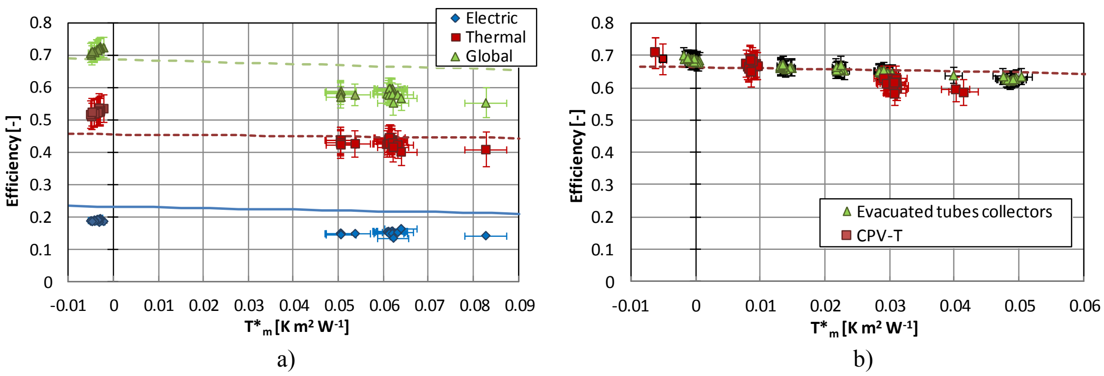

Figure 8. Efficiency vs. reduced temperature difference: measured values (points) and simulated trends (lines) in steady-state conditions. a) With electric load connected. b) Without electric load.

For comparison, in Fig. 8b) thermal efficiency of the present CPVT system is plotted together with the one of an evacuated tubes solar collector, measured in the same laboratory. Although the receiver is not optimized for heat production, the performance of the CPVT system is comparable with that of the evacuated tube collector, due to the low heat dissipations which are associated with the reduced surface area. This result shows the capability of such concentrating devices to produce heat at medium temperature.

Finally, Figure 9 shows a simulation for a clear sky day of June. Inlet water temperature is 85°C. The electric power is around 500 W and the thermal power is around 1250 W for 9 hours. The daily yield of electric energy and heat at 85 °C inlet water temperature are 20.7 MJ and 41.0 MJ, respectively. The estimated average electric, thermal and global efficiencies are 23.1 %, 41.6% and 64.7%, respectively.

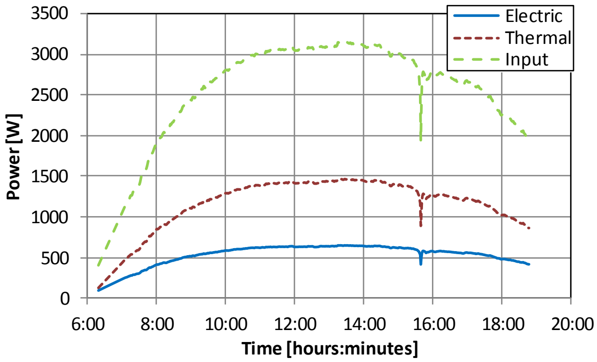

Figure 9. Power vs. local time simulated for June 22, 2012.

8. Concluding remarks

In the present work a CPVT experimental apparatus is described and tested. A model has been developed to predict the electric and thermal production. The electric efficiency displays a minor penalization with increasing reduced temperature difference, therefore it is possible to increase the operating temperature to produce heat at medium temperature (80-90°C). The measured global efficiency reaches 70%.

Acknowledgements

The authors acknowledge the financial support of Regione del Veneto, through the project SMUPR n. 4148 “Polo di Ricerca nel Settore Fotovoltaico”. The present authors want also to thank the company Greenetica srl, Pordenone, Italy for the cooperation within the present project.

References

[1] Del Col D, Dai Prè M, Bortolato M, Padovan A. Investigation of PV solar devices for electricity production and heat recovery. *Proc.. 67° Congresso Nazionale ATI (Trieste)* 2012.

[2] Royne A, Dey CJ, Mills DR. Cooling of photovoltaic cells under concentrated illumination: a critical review. *Solar Energy Materials & Solar Cells* 2005;**86**:451-483.

[3] Chemisana D. Building integrated concentrating photovoltaics: A review. *Renewable and Sustainable Energy Reviews* 2011;**15**:603-611.

[4] Pérez-Higueras P, Muñoz E, Almonacid G and Vidal PG. High Concentrator Photovoltaics efficiencies: Present status and forecast. *Renewable and Sustainable Energy Reviews* 2011;**15**:1810-1815.

[5] Vivar M, Clarke M, Pye J, Everett V. A review of standards for hybrid CPV-thermal systems. *Renewable and Sustaiable Energy Reviews* 2012;**16**:443-448.

[6] European Standard EN 12975-2:2006. Thermal soalr systems and components. Solar collectors-Part 2: test methods.Brussels: CEN; 2006.

[7] ISO GUM standard, Guide to the Expression of Uncertainty in Measurement 1995.

[8] Duffie A, Beckmann WA. *Solar engineering of thermal processes*. 3rd ed. New Jersey:Wiley & Sons; 2006.